

## JET IMPINGEMENT HEAT TRANSFER OF MOVING METAL SHEET

Kulkarni G.A.\* and Specht E.

Author for correspondence

Institute of Fluid Dynamics and Thermodynamics,

Otto-von-Guericke University,

Magdeburg, 39106,

Germany.

E-mail: gaurav.kulkarni@ovgu.de

### NOMENCLATURE

$T$	[ $^{\circ}\text{C}$ ]	Temperature
$s$	[ $m$ ]	Thickness
$\dot{q}$	[ $\text{W}/m^2$ ]	Heat flux
$t$	[ $s$ ]	Time
$x$	[ $m$ ]	Lagrangian length axis
$y$	[ $m$ ]	Lagrangian thickness axis
$z$	[ $m$ ]	Eulerian length axis
$v_c$	[ $m/s$ ]	Casting velocity
$C$	[ $\text{J}/\text{kg}\cdot\text{K}$ ]	Specific heat capacity

#### Special characters

$\lambda$	[ $\text{W}/m\cdot\text{K}$ ]	Thermal conductivity
$\rho$	[ $\text{kg}/m^3$ ]	Density
$\theta$	[-]	Dimensionless temperature

#### Subscripts

$z = 0$	Origin with respect to mold position
1	Pre-cooling region
2	Quenching region
$b$	Final value
0	Initial value
$s$	Start of cooling

### ABSTRACT

This paper reviews the quenching of a moving metal sheet with series of jets from a mold. Experiments were conducted on various samples and the temperature on the back side of the plate was measured using an infrared camera with high local resolution. An analysis method developed by the author was used to obtain heat flux as a function of temperature on the quenching side of the sheet in the steady state region, accounting for the thickness of the sheet. The analysis method is also less sensitive to experimental and numerical errors. The thermal history data is used in conjunction with the analysis method in order to obtain the heat flux and surface temperatures. A study analysing the boiling curve and width of the wetting front is conducted for different metals with different mold moving speeds and initial temperature. The results are compared and analysed for identifying various influencing parameters during the continuous quenching process.

### Motivation

Obtaining the boiling curve is a fundamental requirement for simulation of quenching or metal processing as it determines the rate of cooling. A high cooling rate, would lead to better met-

allurgical properties but deteriorates the mechanical properties. Hence, obtaining an optimum cooling strategy is important. The boiling curve is sensitive to the experimental setup. Hence analysis is conducted on a setup similar to that in industry. In this study, boiling curve along with width of various wetting fronts are analysed for various casting speeds, metals and initial temperatures.

### INTRODUCTION

Quenching with an array of jets is a widely used application in metal casting and in the metal processing industry. During this process, the metal experiences highly non-uniform thermal gradients, which results in thermal stresses and distortions or other forms of defects. Hence quantifying the heat transfer to cooling water is very important for optimization of quenching process. Heat transfer to the cooling water is particularly complicated, due to the phase changing nature of water, typically resulting in the heat extraction rate varying from those associated with transition or film boiling through nucleate boiling to convection.

Large number of researchers have studied the quenching of hot metal sheet. Elias and Yadigaroglu (1977) [1] developed an analytical one-dimensional model for the rewetting of a hot plate and predicted the wetting front velocity. They focussed the importance of axial heat conduction. Wells and Cockcroft (2001) [2] applied an iterative two-dimensional FE inverse heat conduction model to estimate the surface heat flux. The experimental data obtained from thermocouples was smoothed and subsequently used for the inverse model. Nallathambi and Specht (2009) [3] applied a non-iterative finite element method for a two-dimensional inverse heat conduction problem, but it was observed that inverse FE model is very sensitive to experimental and numerical errors causing fluctuations in the results.

Mozumder et al. (2005) [4] studied the delay of wetting front propagation during jet impingement quenching and concluded that the value of maximum heat flux is 5 - 60 times higher than the heat transfer value just before the wetting front movement. Akmal et al. (2008) [5] studied the influence of initial surface temperature, water temperature and jet velocity on curved surface exposed to an impinging water jet.

Beck et al. 1985 [6] used inverse heat conduction technique for estimating heat flux on the surface of a conduction medium through the use of temperature measurements from experiments. Ijaz et al. (2007) [7] have presented an adaptive state estimator for the estimation of input heat flux and measurement sensor bias in a two-dimensional inverse heat conduction problem. Continuous-time analogue hop-field neural network based inverse solution algorithm has been proposed by Hwang (2006) [8] and Deng (2006) [9] and. Gradeck et al. (2011) [10] used temperature data from infrared camera to obtain transient heat flux with an inverse heat conduction problem formulated using an analytical solution of the direct problem expressed in Hankel space.

This paper is primarily focussing on heat transfer during the steady-state region of DC casting process. Cooling because of diffusion is also incorporated as there will be temperature drop before heat transfer to quenching water. The interface temperature and heat flux as a function of position are determined based on 1-D model and 2-D finite difference model respectively, which is used to obtain the heat flux as a function of temperature on quenching side of the plate. In order to identify the parameters influencing the boiling curve, experiments were conducted on metal sheet with varying casting speeds, various metals and metal sheets with different initial temperatures and the data was analysed to obtain heat flux as a function of temperature on quenching side of the sheet.

## Experimental Method

### Setup

An experimental setup, consisting of a mold with an array of jets that creates a water curtain along the surface of metal is used. The dimension of the mold used are 110 mm x 90 mm x 65 mm. It has 8 small orifices at the base, each of 2.4 mm in diameter and forming an angle of 45 to the metal sheet. The experimental setup of this moving mold analysis is shown in Fig. 1. A metal plate is heated to the desired initial temperature and is shifted immediately to the quenching chamber. During the quenching process, an Infra-Red camera is used to capture and store the thermal images at a frame rate of 150 images per second with a resolution of 240 x 80 pixels. The samples were painted black on the measuring side in order to increase the emissivity, for more accurate measurements.

The optical sensor was fixed in front of the hot plate and sends a small electrical signal to be amplified and forwarded to the controller. The latter will activate the DC motor which actuates the axial movement. As mold position is fixed on the axis, the mold will move together along the axis. This movement is relatively similar to the real process, where the ingot or billet is the moving part instead of the mold. The mold moving speed or the casting speed depends on the experimental requirement, which is completely controlled by the DC motor. The cooling water was delivered by a centrifugal pump from the top of the mold and flow out through the array of orifices which produce water jets. These jets impinge on the quenching side of the metal sample. It was

ensured that the same amount of water flowed through every orifice. In the cooling process, the mold moves from the bottom to the top of the sample. A fixed jet velocity of 1.2 m/s was fixed for the experiments.

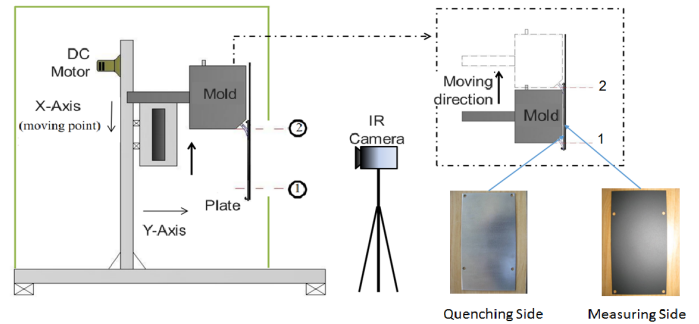


Figure 1. Moving mold mechanism experimental setup

### Experimental Sample

A rectangular sheet of aluminum alloy AA6082, with length and width as 140mm and 70mm respectively and a thickness of 3mm and Nickel and Nicrofer plate with thickness 2mm was used for experimental investigation. The samples were painted black on the measuring side in order to increase the emissivity, for a more accurate measurement. From the emissivity calibration process, it was found that the emissivity of the coating was stable in the range of 0.90 to 0.92 and independent from surface temperature.

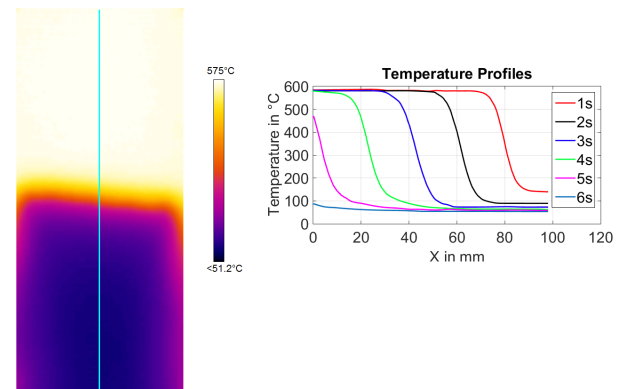


Figure 2. Temperature profiles of metal sheet along the center line for Aluminum with  $v_c = 20\text{mm/s}$

For the purpose of accuracy, the thermal images were captured and stored at an extremely high frame rate of 150 images per second with the resolution of  $240 \times 80$  pixels. Therefore, a temperature analysis can be done for every 0.84 mm and to an accuracy of  $\pm 0.1\text{K}$ . The temperature measurement range of  $50 - 650^{\circ}\text{C}$  was used as low range and  $350 - 1050^{\circ}\text{C}$  was used as high range for this experimental setup. The results along the center line are considered for analysis in order to minimize the errors because of end effects.

Fig. 2 shows an example of thermal image from the infrared

**Table 1.** My caption

	Aluminum	Nickel	Nicrofer
<b>Density</b>	2700 kg/m <sup>3</sup>	8908 kg/m <sup>3</sup>	8400 kg/m <sup>3</sup>
<b>Thermal Conductivity</b>	170 W/m·K	65 W/m·K	17 W/m·K
<b>Specific Heat Capacity</b>	1050 J/kg·K	500 J/kg·K	510 J/kg·K
<b>Thickness</b>	3 mm	2 mm	2 mm

camera during the quenching process. This acquired thermal history data was processed further in order to obtain the temperature data as a function of time and position.

### Analysis Method

A model to obtain the boiling curve developed by the author is used to analyse the results and study the influence of various parameters. A brief description of this method is provided in this section. This method can be applied to the steady state region of experiment. This method is particularly less sensitive to experimental and numerical errors.

The steady state region can be divided mainly in 2 regions, pre-cooling region and quenching region. Pre-cooling region is the region in which heat loss is because of heat diffusion in axial direction. In this region there will be a significant thermal gradient even before the material point experiences water cooling. This region will be particularly significant in materials with high thermal conductivity. Followed by pre-cooling region will be quenching region, where the metal sheet will experience cooling because of quenching water. The distinction between these 2 regions is done by determining the interface temperature using the analytical solution for temperature profile.

An analytical expression for temperature profile in quenching region is determined by curve fitting. This analytical expression is used in conjunction with energy equation to determine the heat flux. The simplified governing differential equations are solved in a two-dimensional finite difference model in order to obtain the heat flux as a function of temperature on quenching side and measuring side of the plate.

### Advection

Preliminary, it is required to distinct between pre-cooling region and the quenching region as seen in Fig. 3. This is done by identifying the interface temperature between these regions or the temperature drop because of diffusion in pre-cooling region. The interface temperature ( $T_{z=0}$ ) is the temperature at the material point transitioning from pre-cooling region to quenching region, this is the temperature where the heat transfer with quenching water begins. Experimentally, it is difficult to distinguish between these regions as there is spluttering when the jet hits the plate. In the pre-cooling region, the thermal gradient along the thickness is not very strong as there is no heat flux on the boundary in this region. Hence, a solution of one-dimensional heat

conduction equation will provide a reasonable temperature profile. Since the plate thickness is small, in the quenching region entire cooling is completed within the impingement zone. Hence distinguishing between free falling zone and impingement zone is not required.

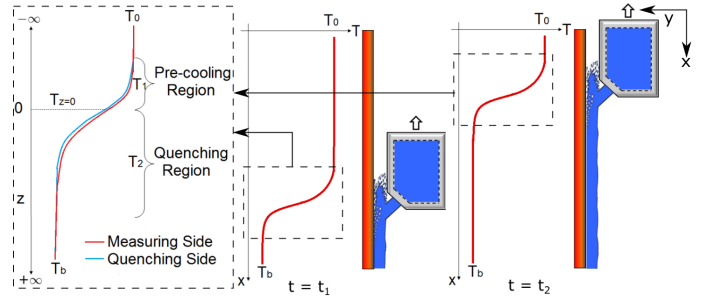


**Figure 3.** Temperature profiles in different regions in quenching process

An one-dimensional conduction equation for solid can be written as:

$$\lambda \frac{\partial^2 T}{\partial z^2} - \frac{\dot{q}}{s} = \rho C \frac{DT}{Dt} \quad (1)$$

where  $\lambda$ ,  $\rho$ ,  $C$ ,  $s$  are thermal conductivity, density, specific heat capacity and thickness of the slab respectively. Also,  $T$  and  $\dot{q}$  are the temperature and heat flux on quenching side of the sheet.

### 0.1 Quasi-Steady State

For a constant casting velocity  $V_c$ , in the spacial vicinity of the mold, the space and time derivatives are then related by:

$$\frac{DT}{Dt} = V_c \frac{\partial T}{\partial z} + \frac{\partial T}{\partial t} \Big|_z \quad (2)$$

Either mold moves relative to laboratory reference, or the plate moves, the temperature profile in the eulerian region in the vicinity of the mold, is nearly independent of time.

$$\frac{\partial T}{\partial t} \Big|_z = 0 \quad (3)$$

This can also be verified with the experimental results when the temperature profile for 20mm/s casting velocity for 2,3,4 seconds, as shown in Fig. 2 are superimposed for the vicinity of the mold. Since the profiles match well, the quasi-steady state assumption is valid, as shown in Fig. 4. The cooling of the sheet because of radiation and natural convection can be neglected, as the heat loss by radiation and natural convection is very small compared to heat loss by cooling water

Using this condition 3, Eq. 2 can be simplified as,

$$\frac{DT}{Dt} = V_c \frac{\partial T}{\partial z} \quad (4)$$

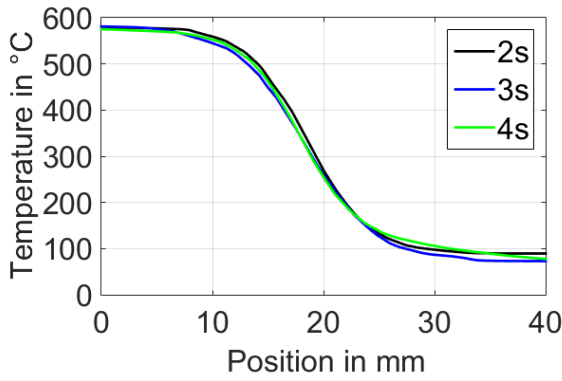


**Figure 4.** Temperature profiles of Aluminum 20mm/s casting velocity

This condition is referred to as quasi steady state condition by Agrawal and Sahu (2013) [11] Using this condition 4, Eq. 1 can be written as:

$$\lambda \frac{\partial^2 T}{\partial z^2} - \frac{\dot{q}}{s} = \rho C V_c \frac{\partial T}{\partial z} \quad (5)$$

The advection term from Eq. 4 will incorporate the movement of the mold. To solve this governing differential equation Eq. 5, we can define following normalized variables:

$$\theta_1 = \frac{T_1 - T_b}{T_{z=0} - T_b} \quad \theta_2 = \frac{T_2 - T_b}{T_{z=0} - T_b} \quad \theta_0 = \frac{T_0 - T_b}{T_{z=0} - T_b} \quad (6)$$

So Eq. 5 will be transformed to as following for the pre-cooling region

$$\frac{d^2 \theta_1}{dz^2} - Pe \frac{d\theta_1}{dz} = 0 \quad (7)$$

and for the quenching region as

$$\frac{d^2 \theta_2}{dz^2} - Pe \frac{d\theta_2}{dz} - Bi \theta_2 = 0 \quad (8)$$

So by assuming a constant Biot number in the quenching region with Sparrow and Siegel approach as used by Yamanouchi 1968 [12] we obtain the following solution:

$$\theta_1 = \theta_0 + (1 - \theta_0) e^{(Pe \cdot z)} \quad (9)$$

$$\theta_2 = e^{\left[ -\frac{Pe}{2} \left( \sqrt{1 + \frac{4 \cdot Bi}{Pe^2}} - 1 \right) \cdot z \right]} \quad (10)$$

where,

$$\theta_0 = \frac{1 + \sqrt{1 + \frac{4 \cdot Bi}{Pe^2}}}{2} \quad (11)$$

With this approach we can determine  $T_{z=0}$  for a constant Biot number in the quenching region and hence distinguish between the pre-cooling region and quenching region.

### 1 Heat flux as a function of position

Since we have quantified the quenching region, the temperature profile in the quenching region can be obtained. An analytical expression for this temperature profile can be obtained by curve fitting. For this *Origin* software was used. It was observed that an Boltzmann function provides the best fit to the experimental temperature profile. The temperature only in the transition region is considered in order to increase accuracy of curve fitting. The equation for the Boltzmann function is as following:

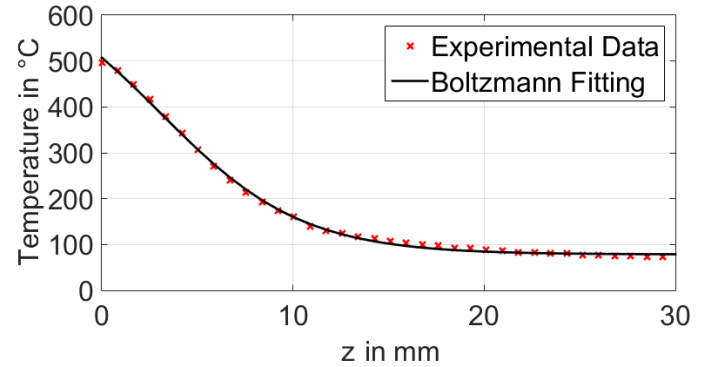


**Figure 5.** Fitting Boltzmann function with experimental temperature profile

$$T = A_2 + \frac{A_1 - A_2}{\left[ 1 + e^{\left( \frac{z - z_0}{dz} \right)} \right]} \quad (12)$$

From Fig. 5, it can be observed that the experimental data matches well with the Boltzmann curve. Hence we can assume this analytical expression for temperature profile as a function of position. Since we have the analytical expression for the temperature distribution, the first and second spatial derivatives can be obtained. So from Eq. 5 we obtain :

$$\dot{q}(z) = s \lambda \frac{\partial^2 T}{\partial z^2} + s V_c \rho C \frac{\partial T}{\partial z} \quad (13)$$

By this method we can obtain an analytical expression of heat flux as a function of position. But in order to obtain boiling curve, it is required to determine heat flux as a function of temperature on quenching side.

## 2 Heat flux as a function of temperature

Even though a thin aluminium sheet is used for experimental analysis, the temperature on the measuring side will be different from the temperature on the quenching side. The difference will be higher specially at DNB temperature since the heat flux is maximum. Hence, a 2-D analysis where the temperature on the quenching side and that on measuring side will be different is required. So considering the quasi-steady state Eq. 5 in global coordinates, the 2-D conduction equation to be solved will be:

$$\rho C V_c \frac{\partial T}{\partial z} = \lambda \left( \frac{\partial^2 T}{\partial z^2} + \frac{\partial^2 T}{\partial y^2} \right) \quad (14)$$

This equation can be solved with a 2D-Finite Difference Model using central difference discretization and by adding ghost points along the boundaries with Neumann boundary condition. On the quenching side the heat flux as a function of position must be applied as boundary condition and on the measuring side and the bottom boundary an insulated boundary condition is considered. On the top boundary the initial temperature is defined.

Boundary condition on the measuring side:

$$\frac{\partial T}{\partial y} = 0$$

on Quenching side:

$$\frac{\partial T}{\partial y} = -\frac{\dot{q}}{\lambda}$$

on the bottom side:

$$\frac{\partial T}{\partial z} = 0$$

on the top side:

$$T = T_0$$

Solving this model we obtain temperature on measuring side and temperature on quenching side and a plot of heat flux vs. temperature on measuring side and temperature on quenching side is obtained, as observed in Fig.6. It can be seen that the temperature on measuring side from the 2D-FD model and the temperature profile measured experimentally are matching, hence the profile of heat flux on the quenching side is consistent and this along side the temperature on the quenching side from the 2D-FD model can be used to obtain the boiling curve.

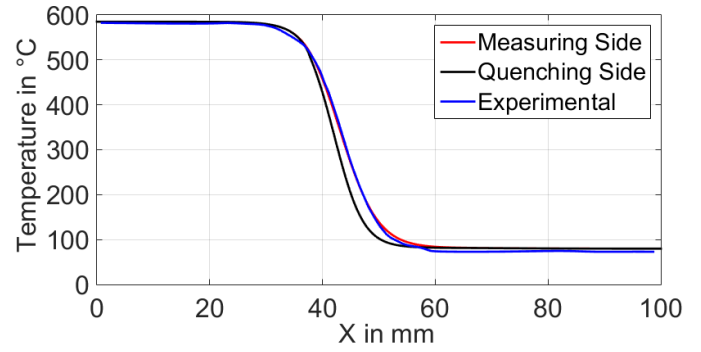


**Figure 6.** Comparison of experimental and 2D-FD model for Al with  $v_c = 20 \text{ mm/s}$

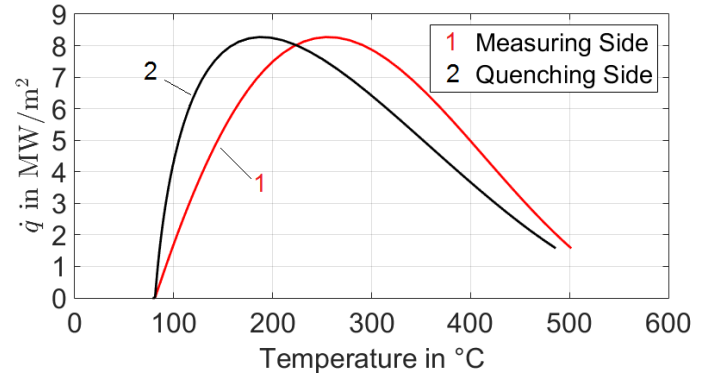


**Figure 7.** Heat flux as a function of temperature on measuring side and quenching side for Al with  $v_c = 20 \text{ mm/s}$

## Results

The thermal history data obtained from the experiments conducted, along with the analysis model was analysed for various parameters. This study was conducted to identify the parameters influencing the heat flux and the respective temperatures. With the proposed model it can be seen from Fig. 8 that even for a thin plate of 3 mm with high thermal conductivity material, the temperature difference at maximum heat flux is of nearly  $80^\circ\text{C}$ . This difference will be even higher in case of low thermal conductivity materials. With a reduction in mold movement speed or casting velocity this difference will be reduced.

Since, an infrared camera is used to measure the temperature, a full field temperature data is generated. These experimental temperature profiles along with the interface temperatures, can be superimposed on each other in order to provide us an preliminary idea of the trend cooling curves that can be expected from the raw experimental data. This data is processed further to obtain the boiling curves and the temperature profile on the quenching side of the metal sheet.

This temperature profile on the quenching side is used to analyse the widths of various wetting front regions. Firstly, a pre-cooling region, this is a region where cooling occurs because of heat transfer in the axial direction to the cool region. The start of this region can be considered when the temperature reaches 99% of initial temperature i.e.  $T_s = 99\%$  of  $T_0$  on the quenching side.

The end of this region can be considered when the temperature on the quenching side reaches the interface temperature  $T_{z=0}$ .

Secondly, transition boiling region, this is the region where the heat flux to quenching water increases with cooling of the metal sheet. In this region the heat flux is because of partial contact between quenching water and hot metal sheet. The start of this region can be considered when the temperature on the quenching side is interface temperature  $T_{z=0}$  and the end will be when the heat flux reaches maximum at DNB temperature  $T_{DNB}$ .

Thirdly, nucleate boiling region, this is the region where heat flux decreases with cooling of metal sheet. Physically this region can be identified by intensive bubble formation on the surface of metal sheet. The start of this region can be considered when the temperature on the quenching side is DNB temperature  $T_{DNB}$  and the end can be considered when the temperature reaches  $100^{\circ}\text{C}$ .

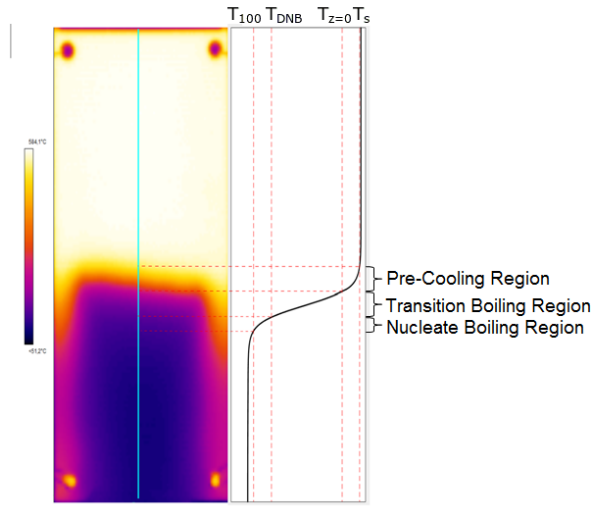


Figure 8. Width of various regions for Al with  $v_c = 20\text{mm/s}$

**Different Casting Speeds**

In order to quantify the influence of casting speed on the cooling of a metal sheet, an Aluminum sheet was used. This sheet was heated to a temperature of nearly  $575^{\circ}\text{C}$  and was quenched with different moving speeds and the superimposed temperature profiles Fig. 9, boiling curves Fig. 10 and front widths Tab. 2 were analysed. It can be observed that with increase in casting speeds, the interface temperature increases along with the maximum heat flux. The width of pre-cooling region decreases with increasing casting velocities.

**Different Metals**

To identify how the heat transfer during quenching changes for different metals, experiments were conducted with Aluminum, Nickel and Nicrofer. These metals were selected because of their diverse material properties. These sheets were heated to a temperature of nearly  $575^{\circ}\text{C}$  and were quenched with mold mov-

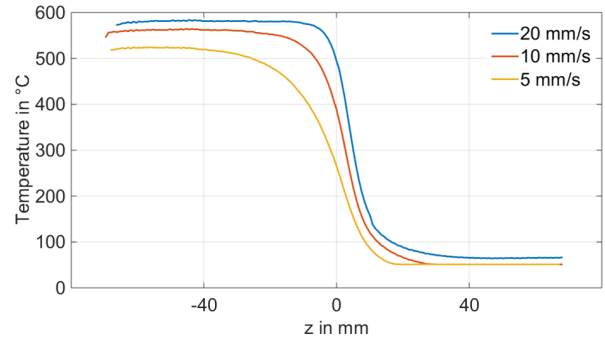


Figure 9. Temperature profiles from the raw experimental data superimposed for different casting speeds.

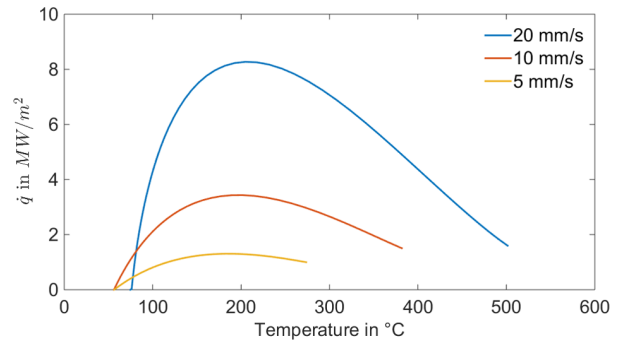


Figure 10. Boiling curves for different casting speeds

	20 mm/s	10 mm/s	5 mm/s
<b>Pre-cooling Region</b>	7.75 mm	22.64 mm	40.90 mm
<b>Transition Boiling Region</b>	7.70 mm	5.87 mm	3.49 mm
<b>Nucleate Boiling Region</b>	5.01 mm	5.86 mm	7.48 mm

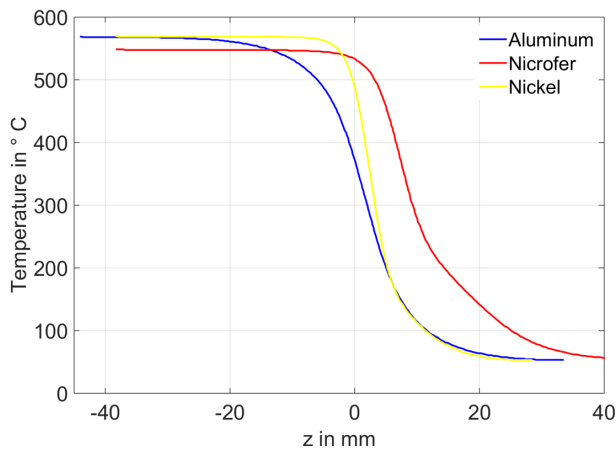
$T_s = 0.99 \cdot T_0$	$579^{\circ}\text{C}$	$554.4^{\circ}\text{C}$	$519.7^{\circ}\text{C}$
$T_{z=0}$	$498^{\circ}\text{C}$	$387.9^{\circ}\text{C}$	$270.7^{\circ}\text{C}$
$T_{dnb}$	$205^{\circ}\text{C}$	$195^{\circ}\text{C}$	$190^{\circ}\text{C}$

Table 2. Front width for different casting speeds

ing speed on  $10\text{mm/s}$  and the superimposed temperature profiles Fig. 11, boiling curves Fig. 12 and front widths Tab. 2 was analysed. It can be observed that the decrease in temperature in pre-cooling region is small in case of Nicrofer because of low thermal conductivity compared to Nickel and Aluminum.

**Different Initial Temperatures**

Initial temperature is also thought to have an influence on heat flux during quenching of metal sheet. To quantify this influence, experiments were conducted on a Nickel sheet with casting speed



**Figure 11.** Temperature profiles from the raw experimental data superimposed for different metals.

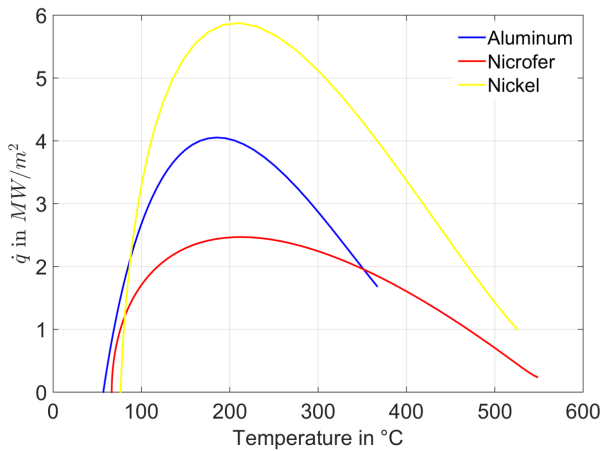


**Figure 12.** Boiling curves for different metals

of 10mm/s and an initial temperatures of nearly 575°C and of 785°C. For temperature of 785°C, experiments were repeated with a high temperature range and low temperature range setting in the Infrared camera. These 2 temperature range data were combined to obtain the raw data for the entire quenching process. The superimposed temperature profiles Fig. 13, boiling curves Fig. 14 and front widths Tab. 2 were analysed. It can be seen that the boiling curve is different for different initial temperatures.

**CONCLUSION**

A model which takes into account the temperature difference on quenching side and measuring side of the metal sheet along with the pre-cooling caused by diffusion is used to obtain the boiling curve in the steady state region of moving metal sheet. Various experiments were conducted to identify the influencing parameters.

It can be observed that metals with high thermal conductivity, have a longer pre-cooling region and this region is even longer when the casting speed is lower. In metal casting and processing industry, it is required that the cooling rate should be greater than

	Nicrofer	Nickel	Aluminum
<b>Pre-cooling Region</b>	2.01 mm	3.68 mm	22.64 mm
<b>Transition Boiling Region</b>	13.37 mm	4.34 mm	5.87 mm
<b>Nucleate Boiling Region</b>	5.36 mm	3.01 mm	5.86 mm

$T_s = 0.99 \cdot T_0$	548.65 °C	565.48 °C	554.4 °C
$T_{z=0}$	533.42 °C	486.38 °C	387.9 °C
$T_{dnb}$	214.3 °C	211.7 °C	195 °C

**Table 3.** Front width for different metals

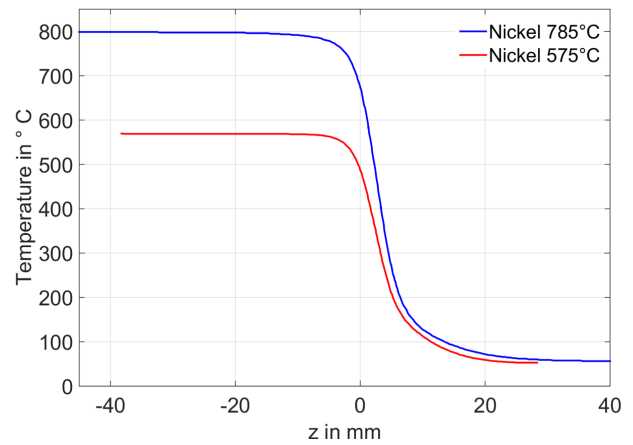


**Figure 13.** Temperature profiles from the raw experimental data superimposed for different initial temperatures.

critical cooling rate in order to obtain good material properties. With the obtained results it can be concluded that a higher metal sheet moving speed should be maintained in order to minimize the slow cooling in the pre-cooling region. Though this increases the length of the quenching setup, the pre-cooling region can be minimized. Also it should be noted that the high cooling rate increases the thermal gradients in metal increasing the thermal stresses. This might lead to failure in the metal and hence an optimized cooling rate should be determined and used.

DNB temperature or the temperature where the heat flux is maximum is in the range of nearly 200°C - 215°C for an initial temperature of 575°C despite of various casting speeds and different kinds of metals. This phenomenon has been observed and published by many authors. For higher initial temperature, the DNB temperature also is higher. It can be observed that the maximum heat flux, decreases for decreasing casting velocity. Nickel demonstrates a higher maximum heat flux compared to Aluminum and Nicrofer. It can also be observed that the initial temperature also has a strong influence on the maximum heat flux for a metal sheet. This could also explain the difference in max-

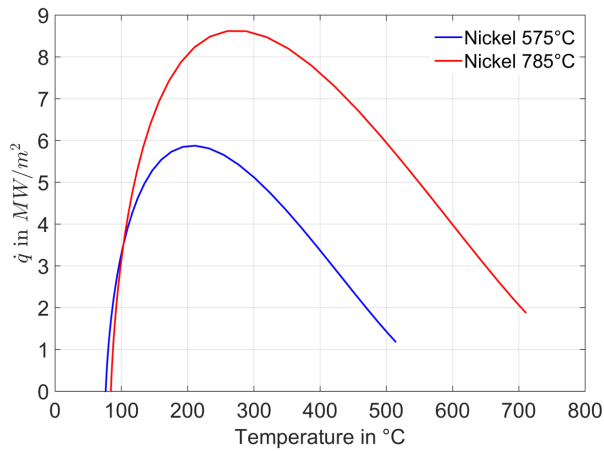


**Figure 14.** Boiling curves for different initial temperatures

	Nickel 575 °C	Nickel 785 °C
<b>Pre-cooling Region</b>	3.68 mm	3.84 mm
<b>Transition Boiling Region</b>	4.34 mm	4.53 mm
<b>Nucleate Boiling Region</b>	3.01 mm	4.01 mm

$T_s = 0.99 * T_0$	565.48 °C	789.99 °C
$T_{z=0}$	486.38 °C	675.04 °C
$T_{dnb}$	211.7 °C	259.8 °C

**Table 4.** Front width for different initial temperatures

imum heat flux for different casting speeds as the temperature at which metal sheet will experience water cooling will vary.

## REFERENCES

[1] Elias, E. and Yadigarogul, G., A General one-dimensional Model for Conduction-Controlled Rewetting of a Surface, *Nuclear Engineering and Design*, Vol. 42, No. 2, 1977, pp. 185-194

- [2] Wells, M. A. and Li, D. and Cockcroft, S. L., Influence of Surface Morphology, water flow rate and sample thermal history on the boiling-water heat transfer during Direct-chill casting of commercial aluminum alloys, *Metallurgical and Materials Transactions B*, Vol. 32B, 2001, pp. 929-939
- [3] Nallathambi, A. K. and Specht, E., Estimation of heat flux in array of jets quenching using experimental and inverse finite element method, *Journal of Materials Processing Technology*, Vol. 209, 2009, pp. 5325-5332
- [4] Mozumder, A. K. and Monde, M. and Woodfield, P. L., Delay of wetting propagation during jet impingement quenching for a high temperature surface, *International Journal of Heat and Mass Transfer*, Vol. 48, 2005, pp. 5395-5407
- [5] Akmal, M. and Omar, A. M. T. and Hamed, M. S., Experimental investigation of propagation of wetting front on curved surfaces exposed to an impinging water jet, *International Journal of Microstructure and Materials Properties*, Vol. 3, 2008, pp. 645-681
- [6] Beck, J. -V. and Blackwell, B. and St-Clair, C. -R., *Inverse Heat Conduction - Ill-Posed Problems*, Wiley, New York, 1985
- [7] Ijaz, U. Z. and Khambampati, A. K. and Kim, M. C. and Kim, S. and Kim, K. Y., Estimation of time-dependent heat flux and measurement bias in two-dimensional inverse heat conduction problems, *International Journal of Heat and Mass Transfer*, Vol. 50, 2007, pp. 4117-4130
- [8] Huang, C. H. and Wu, H. H., An inverse hyperbolic heat conduction problem in estimating surface heat flux by conjugate gradient method, *Journal of Physics D-Applied Physics*, Vol. 39, 2006, pp. 4087-4096
- [9] Deng, S. and Hwang, Y., Applying neural networks to the solution of forward and inverse heat conduction problems, *International Journal of Heat and Mass Transfer*, Vol. 42, 2006, pp. 4732-4750
- [10] Gradeck, M. and Quattara, J. A. and Rémy, B. and Maillet, D., Solution of an inverse problem in the Hankel space Infrared thermography applied to estimation of a transient cooling flux, *Experimental Thermal and Fluid Science*, Vol. 36, 2012, pp. 56-64
- [11] Agrawal, M. K. and Sahu, S. K., Analysis of conduction-controlled rewetting of a hot surface by variational method, *Heat Mass Transfer*, Vol. 49, 2013, pp. 963-971
- [12] Atsuo Yamanouchi, Effect of Core Spray Cooling in Transient State after Loss of Coolant Accident, *Journal of Nuclear Science and Technology*, Vol. 5, No. 11, 1968, pp. 547-558